J Supercond Nov Magn (2013) 26:1625–1630
DOI 10.1007/s10948-012-1913-6

ORIGINAL PAPER

Structural and Electrical Properties of Monovalent Doped Manganites $Pr_{0.6}Sr_{0.4-x}K_xMnO_3$ ($x = 0$, 0.05 and 0.1)

R. Thaljaoui · W. Boujelben · M. Pękała · K. Pękała · A. Cheikhrouhou

Received: 6 November 2012 / Accepted: 30 November 2012 / Published online: 22 December 2012

Abstract Structural and electrical properties of the mixed-valence monovalent doped manganites $Pr_{0.6}Sr_{0.4-x}K_xMnO_3$ ($x = 0$, 0.05 and 0.1), prepared using the conventional solid-state synthesis method, have been investigated. Rietveld refinement of the X-ray diffraction patterns at room temperature shows a slight increase in unit cell volume with K content and confirms that all powder samples are single phase and crystallize in the orthorhombic structure with *Pnma* space group. Electrical resistivity measurements under and without magnetic field show a transition from the metallic to insulating behavior. The electrical conductivity is improved with increasing K content. The resistivity data in metallic region were fitted according to the electron–electron scattering process while in insulating region they were fitted using the small polaron hopping SPH model and Mott's variable range hopping VRH model.

Keywords Perovskite manganites · Magnetic properties · Magnetoresistance effect

R. Thaljaoui · W. Boujelben (✉) · A. Cheikhrouhou
Laboratoire de Physique des Matériaux, Faculté des Sciences de Sfax, Université de Sfax, B.P. 1171, 3000 Sfax, Tunisia
e-mail: Wahiboboujelben@yahoo.fr

R. Thaljaoui · M. Pękała
Department of Chemistry, University of Warsaw, Al. Zwirki i Wigury 101, 02-089 Warsaw, Poland

R. Thaljaoui · K. Pękała
Faculty of Physics, Warsaw University of Technology, Koszykowa 75, 00-662 Warsaw, Poland

A. Cheikhrouhou
Institut NEEL, CNRS, B.P.166, 38042 Grenoble Cedex 9, France

1 Introduction

Present interest in mixed-valence manganese perovskites with general formula $T_{1-x}R_xMnO_3$ (T = rare-earth cation, R = alkaline earth cation) is related to their colossal magnetoresistance (CMR), and their potential technological application [1–3]. These compounds are characterized due to their sensory electronic and magnetic properties, which are dependent on mobile charge carriers, spin ordering, orbital hybridization. The substitution in the A-site influences the electronic and magnetic properties [4, 5]. Zener showed that the metallic and ferromagnetic behavior in manganite can be explained using the so called double exchange mechanism (DE) [6] with mobile electrons e_g traveling between the Mn^{3+} and Mn^{4+} cations. However, it was suggested that the DE model is not enough to explain the CMR phenomenon. Some authors suggested that other factors such as Jahn Teller [7], phase separation [8–10] are responsible for the behavior observed in manganite. Several studies have been performed on the effect of substitution in the A-site by divalent elements (Ba, Ca) [11, 12]. Recently some authors have reported that the substitution by monovalent element can improve physical properties [13].

In previous studies we have reported that the $Pr_{0.6}Sr_{0.35}Na_{0.05}MnO_3$ exhibits a metal–insulator behavior about 165 K [14, 15]. There have been no previous studies on the effect of monovalent K-doping effect in the $Pr_{0.6}Sr_{0.4-x}K_xMnO_3$ system. Each K atom converts Mn^{3+} ion to Mn^{4+} and varies the Mn^{3+}/Mn^{4+} ratio. This results in a larger charge carrier density due to the difference between the valence of K^+ and Sr^{2+} ions. In the present paper we are reporting a systematic investigation of structural and electrical properties of monovalent K-doped series of manganites with chemical compositional $Pr_{0.6}Sr_{0.4-x}K_xMnO_3$ ($x = 0$, 0.5 and 0.1).

2 Experimental

Polycrystalline samples of $Pr_{0.6}Sr_{0.4-x}K_xMnO_3$ ($x = 0$, 0.05 and 0.1) were prepared using the conventional solid-state reaction method. Stoichiometric ratio of Pr_6O_{11}, $SrCO_3$, K_2CO_3 and MnO_2 (99.9 %) was mixed in an agate mortar and then heated in air to 1000 °C for 60 h with intermediate grinding. The obtained mixtures were then pressed into pellets and sintered at 1100 °C in air for 60 h with intermediate regrinding. Phase purity, homogeneity and cell dimensions were checked by X-ray diffraction studies at room temperature with Cu-Kα radiation (1.54 Å) in the 2θ range of 10–80 degrees. Structural analysis was carried out using the standard Rietveld technique [16, 17]. The dc magnetization was measured in a field of 100 Oe. The electrical resistivity versus temperature was measured by the four probe technique under zero field and a magnetic field of 1 T.

3 Structure

The X-ray diffraction patterns of $Pr_{0.6}Sr_{0.4-x}K_xMnO_3$ ($x = 0$, 0.05 and 0.1) shown in Fig. 1A confirms that all manganites studied can be indexed in the orthorhombic structure with *Pnma* space group without any traces of secondary phases. Figure 1B shows a typical plot of the refined pattern for $x = 0.1$. Structural parameters obtained using Rietveld analysis of the powder XRD data are given in Table 1. It is worth to notice that the unit cell volume is found to increase with increasing K content. This volume enhancement is due to the larger ionic radius of K^+ (1.64 Å) as compared to that of Sr^{2+} (1.44 Å) [18]. A similar tendency is also observed value for other monovalent doped Na-doped manganites with the Na^+ ionic radius of 1.39 Å [14]. It is worth to notice that the Mn–O–Mn angles are enhanced with K doping, whereas the Mn–O distances are slightly suppressed.

The average crystallite size evaluated from a width of diffraction peaks using the Scherrer formula is found to be 41, 49 and 52 nm for $x = 0$, 0.05 and 0.1, respectively. We should note that this value is slightly larger than observed value for Na-doped $Pr_{0.6}Sr_{0.35}Na_{0.05}MnO_3$ manganite [14].

4 Magnetic Properties

The magnetization measured in a field of 100 Oe confirms the ferromagnetic ordering of the manganites studied (Fig. 2). The low temperature magnetization becomes reduced with raising K content due to the enhanced Mn^{4+}/Mn^{3+} ratio. The Curie temperature determined by the dM/dT minimum (not plotted) shifts from 310 K down to 296 K for x varying from 0 to 0.1. It is worth to notice that these Curie temperatures exactly coincide with those reported for the poly- and single crystalline $Pr_{0.6}Sr_{0.4}MnO_3$ manganites [19, 20].

5 Electrical Properties

The absolute values of electrical resistivity varied between 1.2 and 1.4 mΩ m at room temperature for our samples. Temperature dependence of electrical resistivity $\rho(T)$ plotted in Fig. 3 indicates a changeover from the low temperature metallic-like behavior ($d\rho/dT > 0$) below T_ρ to the semiconductor-like ($d\rho/dT < 0$) above T_ρ temperature corresponding to the maximum value of resistivity at $H = 0$ T. The T_ρ temperature diminishes from 184 down to 170 K, when K content x varies from 0 to 0.1.

The T_ρ temperature is more than 100 K lower than the Curie temperature. Such a difference was reported for numerous manganites. The T_ρ temperature is found to depend on a microstructure of the manganite as shown for the nanocrystalline manganites studied with the poly- and single crystalline ones [19, 20]. In the $Pr_{0.6}Sr_{0.4}MnO_3$ single crystal the metallic behavior was observed up to 400 K and the temperature derivative of resistivity has a maximum at Curie temperature [20].

In Fig. 4 we have plotted the temperature dependence of the electrical resistivity measured at 0 and 1 T magnetic field. We observe a reduction in resistivity magnitude seen in a whole temperature range for $H = 1$ T. This observation suggests that potassium facilitates electrical conductivity most probably within the grain boundaries, which was also found in various oxide materials. Magnetic field of 1 T shifts T_ρ to about 194 K almost independently of x.

Electrical resistivity in ferromagnetic metallic phase (below T_ρ) was numerically fitted by the formula

$$\rho(T) = \rho_0 + AT^2 \tag{1}$$

where ρ_0 is a temperature independent low temperature resistivity due to the scattering by impurities, grain boundaries, domain walls [21]. The A term is ascribed to the electron-electron or single magnon scattering [22, 23]. The obtained values from the best fit of resistivity data are summarized in Table 2. The ρ_0 and parameters are found to decrease with increasing K content. The observed reduction of A parameter by a magnetic field of 1 T can be explained by the weakening of spin fluctuation in a presence of external field.

The temperature dependence of electrical resistivity in semiconducting phase (above T_ρ) was analyzed and compared with the Small Polaron Hopping (SPH) and Mott's Variable Range Hopping (VRH) models [24, 25]. For the SPH model, the electrical resistivity can be approximated by the following equation:

$$\rho = BT\exp(E_a/k_BT) \tag{2}$$

where E_a is the activation energy and B is a constant. According to the VRH model the electrical resistivity is expressed by the formula

$$\rho = R\exp(T_0/T)^{1/4} \tag{3}$$

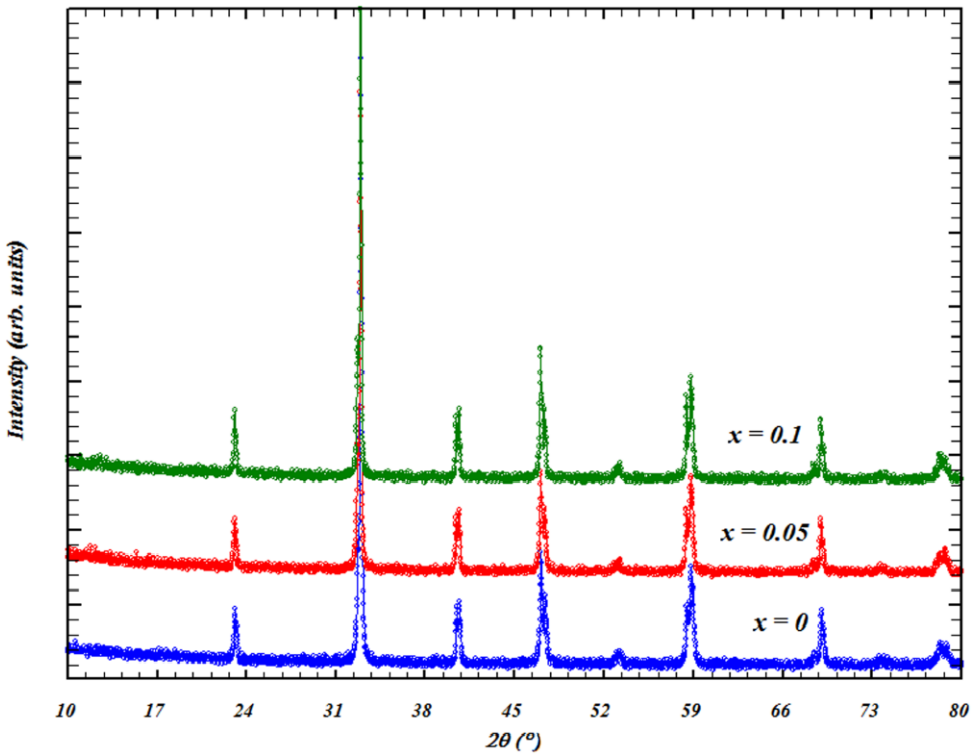

(a)

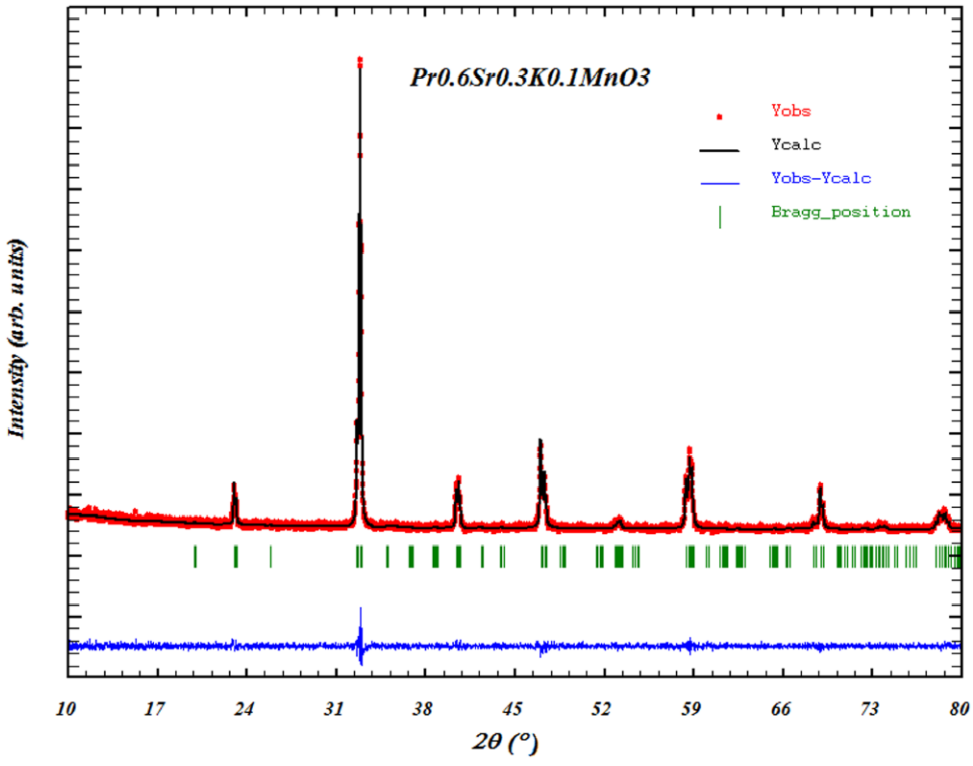

(b)

Fig. 1 (**a**) The X-ray diffraction pattern of $Pr_{0.6}Sr_{0.4-x}K_xMnO_3$ ($x = 0$, 0.05 and 0.1). (**b**) The indexed X-ray diffraction pattern of $Pr_{0.6}Sr_{0.}K_{0.1}MnO_3$

Table 1 Structural data of $Pr_{0.6}Sr_{0.4-x}K_xMnO_3$ ($x = 0$, 0.05 and 0.1)

Parameters	$x = 0$	$x = 0.05$	$x = 0.1$
a (Å)	5.4422	5.4426	5.4427
b (Å)	7.6744	7.6775	7.6783
c (Å)	5.4856	5.4838	5.4839
V (Å^3)	229.108(1)	229.143(6)	229.174(9)
Mn–O_1 (Å)	1.948(5)	1.947(6)	1.946(9)
Mn–O_2 (Å)	1.984(8)	1.967(1)	1.9601(2)
Mn–O_2 (Å)	1.961(8)	1.957(1)	1.951(4)
Mn–O_1–Mn (°)	159.897(8)	161.841(1)	161.89(8)
Mn–O_2–Mn (°)	162.99(4)	163.301(1)	163.85(3)
$\chi 2$	1.25	1.17	1.26
Crystallite size (nm)	41	49	52

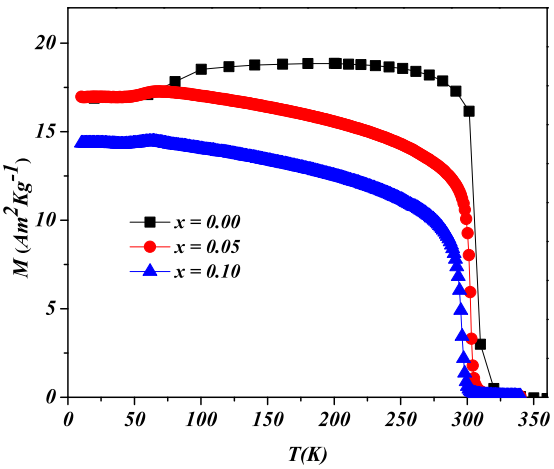

Fig. 2 Temperature variation of magnetization $M(T)$ for $Pr_{0.6}Sr_{0.4-x}K_xMnO_3$ manganite measured in a field of 100 Oe

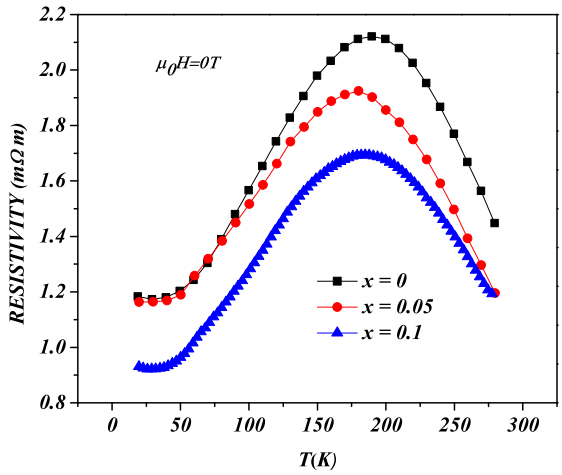

Fig. 3 Temperature dependence of electrical resistivity of $Pr_{0.6}Sr_{0.4-x}K_xMnO_3$ ($x = 0$, 0.05 and 0.1) measured in zero magnetic field

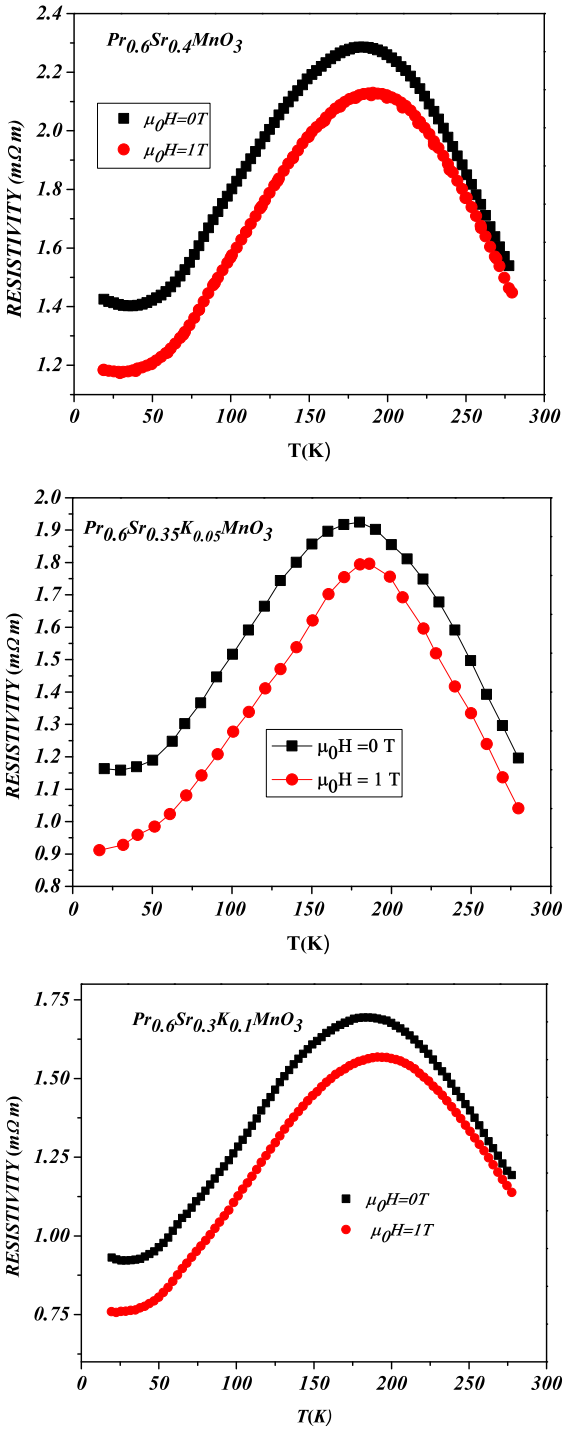

Fig. 4 Temperature dependence of electrical resistivity of $Pr_{0.6}Sr_{0.4-x}K_xMnO_3$ ($x = 0$, 0.05 and 0.1) measured in magnetic applied field of 0 and 1 T

where R is the Mott residual resistivity and T_0 the Mott characteristic temperature related to carrier localization length [25]. The collected resistivity data were fitted by the two above models and the resulting parameters are listed in Table 3. The reliability factors are very close for both models

Table 2 Electrical resistivity fitting parameters in metallic phase of $Pr_{0.6}Sr_{0.4-x}K_xMnO_3$ ($x = 0$, 0.05 and 0.1)

x	ρ_0 (mΩ m)		A (10^{-5} mΩ m K^{-2})	
	$H = 0$ T	$H = 1$ T	$H = 0$ T	$H = 1$ T
0	1.38	1.33	5.16	2.8
0.05	1.17	0.97	3.36	2.96
0.1	0.91	0.81	3.57	2.01

Table 3 Electrical resistivity fitting parameters in semiconducting phase of $Pr_{0.6}Sr_{0.4-x}K_xMnO_3$ ($x = 0$, 0.05 and 0.1)

x	T_0 (10^5 K)		E_a (meV)	
	$H = 0$ T	$H = 1$ T	$H = 0$ T	$H = 1$ T
0	8.10	4.59	75	68
0.05	7.07	5.71	68	59
0.1	5.41	4.35	63	57

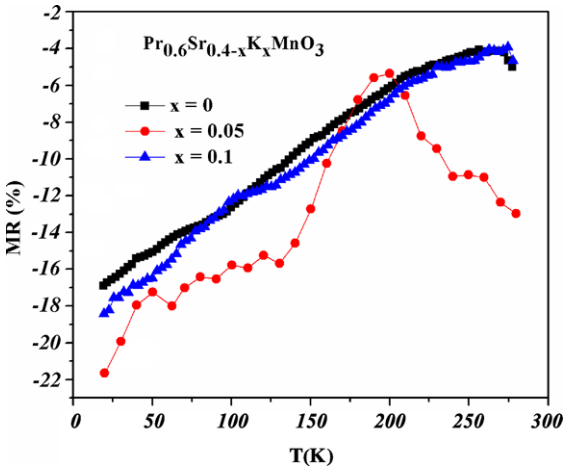

Fig. 5 Temperature dependence of magnetoresistance of $Pr_{0.6}Sr_{0.4-x}K_xMnO_3$ samples

tested and they do not point to the better one. The obtained values of E_a and T_0 from the fitting (Table 3) are characteristic for manganites and decrease with increasing the magnetic applied field to 1 T. Such behavior can be attributed to the suppression of the transport energy barriers under the influence of magnetic field. The derived activation energies E_a are characteristic for manganites. The T_0 values coincide with those reported for $La_{0.85}Ag_{0.15}MnO_3$ [26].

The coexistence of ferromagnetism and metallic conductivity causes the relatively strong effect of negative magnetoresistance (MR) in manganites. The negative magnetoresistance effect is defined as

$$\mathrm{MR} = \frac{\Delta\rho}{\rho} = \frac{\rho(H) - \rho(0)}{\rho(0)} \tag{4}$$

where $\rho(H)$ and $\rho(0)$ are the resistivities at magnetic field H and at zero field, respectively. Figure 5 shows the temperature evolution of MR for an applied magnetic field of 1 T for all our samples. For $x = 0$ and 0.1 the MR reaches about 17 to 19 % at 20 K and gradually decays around room temperature. The MR plot for $x = 0.05$ is distinguished by a peak at 200 K. In contrast to the single crystal of $Pr_{0.6}Sr_{0.4}MnO_3$ manganite [20] the manganites studied do not exhibit MR peak in vicinity of Curie temperature. The strong MR effect observed at low temperature can be related the extrinsic MR effect involving spin polarized tunneling between grains or spin dependent scattering of polarized electrons at grain boundaries [14].

Summarizing one may notice that the $Pr_{0.6}Sr_{0.4-x}K_xMnO_3$ manganites retain the orthorhombic structure up to 10 % potassium doping. The electrical conductivity becomes improved by K doping and the T_ρ temperature is shifted more than 100 K than below the Curie temperature. The negative magnetoresistance effect attains 17 to 22 % at 20 K depending on composition.

References

1. Jin, S., Tiefel, T.H., McCormack, M., Fastnacht, R.A., Ramesh, R., Chen, L.H.: Science **264**, 413 (1994)
2. Rao, C.N., Raveau, B.: Colossal Magnetoresistance, Charge Ordering and Related Properties of Manganese Oxides. World Scientific, Singapore (1998)
3. Tokura, Y., Tomioka, T.: J. Magn. Magn. Mater. **200**, 1 (1999)
4. Raveau, B., Maignan, A., Caignaert, V.: J. Solid State Chem. **117**, 424 (1995)
5. Tomioka, Y., Asamitsu, A., Moritomo, Y., Kowahara, H., Tokura, Y.: Phys. Rev. Lett. **74**, 5108 (1995)
6. Zener, C.: Phys. Rev. **82**, 403 (1951)
7. Millis, A.J., Shraiman, B.I., Muller, R.: Phys. Rev. Lett. **77**, 175 (1996)
8. Schiffer, P., Ramirez, A.P., Bao, W., Cheong, S.-W.: Phys. Rev. Lett. **75**, 3336 (1995)
9. Kalyana Lakshmi, Y., Venugopal Reddy, P.: J. Alloys Compd. **470**, 67 (2009)
10. Rao, G.N., Saibal Roy, R.C., Yang, Chen, J.W.: J. Magn. Magn. Mater. **260**, 375 (2003)
11. Suresh Kumar, V., Mahendiran, R.: Solid State Commun. **150**, 1445 (2010)
12. Kolat, V.S., Izgi, T., Kaya, A.O., Bayri, N., Gencer, H., Atalay, S.: J. Magn. Magn. Mater. **322**, 427 (2010)
13. Das, S., Dey, T.K.: J. Phys. D, Appl. Phys. **40**, 1855 (2007)
14. Thaljaoui, R., Boujelben, W., Pękała, M., Szydłowska, J., Cheikhrouhou, A.: J. Alloys Compd. **526**, 98 (2012)
15. Thaljaoui, R., Boujelben, .W., Pękała, M., Pociecha, D., Szydłowska, J., Cheikhrouhou, A.: J. Alloys Compd. **530**, 138 (2012)
16. Rietveld, H.M.: J. Appl. Crystallogr. **2**, 65 (1969)
17. Roisnel, T., Rodriguez-Carvajal, J.: Computer program FULLPROF, LLB-LCSIM, May 2003
18. Shanon, R.D.: Acta Crystallogr., A Cryst. Phys. Diffr. Theor. Gen. Crystallogr. **32**, 751 (1976)
19. Chang, C.W., Lin, J.G., Tai, M.F.: Chin. J. Phys. **40**, 570 (2002)
20. Rössler, S., Harikrishnan, S., Naveen Kumar, C.M., Bhat, H.L., Suja, E., Rössler, U.K., Steglich, F., Wirth, S.: J. Supercond. Nov. Magn. **22**, 205 (2009)

21. Snyder, G.J., Hiskes, R., Dicarolis, S., Beasley, M.R., Geballe, T.H.: Phys. Rev. B **53**, 14434 (1996)
22. Ziese, M.: Phys. Rev. B **62**, 1044 (2000)
23. Jaime, M., Lin, P., Salamon, M.B., Han, P.D.: Phys. Rev. B **58**, R5901 (1998)
24. Emin, D., Holstein, T.: Ann. Phys. **53**, 439 (1969)
25. Mott, N.F.: Metal–Insulator Transition, p. 51. Taylor and Francis, London (1990)
26. Ibrahim, N., Yahya, A.K., Rajput, S.S., Keshri, S., Talari, M.K.: J. Magn. **323**, 2179 (2011)